ELSEVIER

Journal of Power Sources 92 (2001) 157–162

JOURNAL OF POWER SOURCES

www.elsevier.com/locate/jpowsour

Synthesis of composite metal hydride alloy of A_2B and AB type by mechanical alloying

Sang Soo Han*, Nam Hoon Goo, Woon Tae Jeong, Kyung Sub Lee

Department of Materials Science and Engineering, Hanyang University, 133-791 Seoul, South Korea

Received 28 April 2000; accepted 1 June 2000

Abstract

A composite alloy composed of Mg_2Ni and TiNi phases has been synthesized directly from elemental powders of Mg, Ni and Ti by mechanical alloying. The alloyed powders are produced by milling for 20 h. Most of the powders are not a perfect composite state but a mixture of Mg_2Ni and TiNi grains. The amount of the Mg_2Ni phase is relatively less than that of the TiNi phase because more Mg forms a solid-solution with TiNi than Ti forms with Mg_2Ni. The maximum discharge capacity of the composite electrode is 380 mAh g^{-1} at a discharge current density of 10 mA g^{-1}. This value is higher than that of a mechanically alloyed Mg_2Ni electrode. The composite electrode shows improved cycle-life compared with single-phase Mg_2Ni. For example, after 150 cycles the ratio of the discharge capacity to the maximum value is about 55% whilst the ratio for Mg_2Ni is below 10%. The composite electrode also has a high-rate discharge capability which is about 100 mAh g^{-1} after 40 cycles, regardless of the discharge current density.

Keywords: Composite metal hydride alloy; Mg_2Ni; TiNi; Mechanical alloying

1. Introduction

The specific capacity and specific energy of hydride electrode materials depend on the chemical composition and crystalline structure. Well-known hydrogen-storage materials include AB, A_2B, AB_2 and AB_5 type intermetallic compounds. The corrosion stability of these materials is ascribed to the formation of a passive film on the surface of the material, which can protect the bulk from being further corroded during repeated charging–discharging. If, however, the film is too compact to allow hydrogen to diffuse into and out of the electrode, or if it has a low catalytic activity for the electrochemical reduction and oxidation of hydrogen, the attainable charge–discharge rates, as well as the energy and power densities, are significantly reduced. The characteristics of the electrode surface also determine the rate at which fresh electrodes can be activated.

For a given electrode material, it is difficult to satisfy all the requirements necessary to produce an electrode with maximum performance. In order to overcome this problem, composite hydride materials have been introduced as a new class of electrode materials [1–5]. The composite is a material which consists of two or more hydrogen-storage alloys or intermetallic compounds. The major component is, in general, characterized by good hydrogen-storage properties and high corrosion resistance and, therefore, acts as the main hydrogen-storage medium. The minor component is used as a surface activator to improve the kinetics of hydrogen sorption–desorption, as well as to ease the initial activation of the major component.

Cui et al. [1] successfully synthesized a new composite alloy Mg_2Ni-40 wt.%Ti_2Ni by a particle inlaying method which included mechanical alloying and sintering. It was shown that the discharge capacity of the electrode was effectively improved from 8 mAh g^{-1} for Mg_2Ni to l65 mAh g^{-1} for the new composite electrode at ambient temperature. Terzieva et al. [2] also synthesized Mg-$LaNi_5$ composite materials to improve the absorption–desorption characteristics of magnesium towards hydrogen.

Until recently, all preparations of composite metal hydrides were composed of the following two steps: (i) mechanical milling of each metal hydride and (ii) heat-treatment. These methods are very complex. In our study, the composite metal hydride is very simply synthesized by mechanical alloying of the elemental powders. Thus,

* Corresponding author. Tel.: +82-2-2281-4914; fax: +82-2-2281-4914.
E-mail address: mithan@dreamwiz.com (S.S. Han).

0378-7753/01/$ – see front matter
PII: S0378-7753(00)00516-4

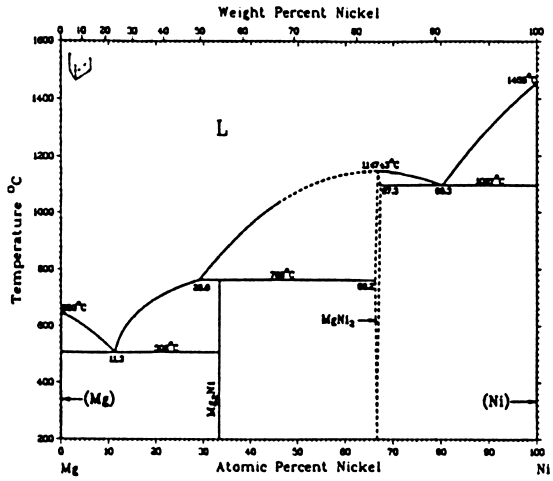

(a) Mg–Ni

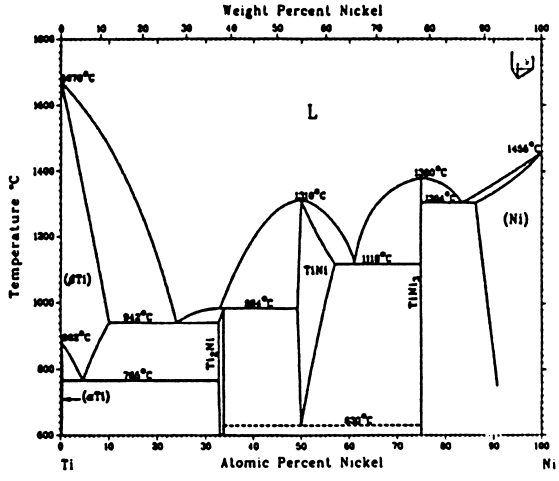

(b) Ti–Ni

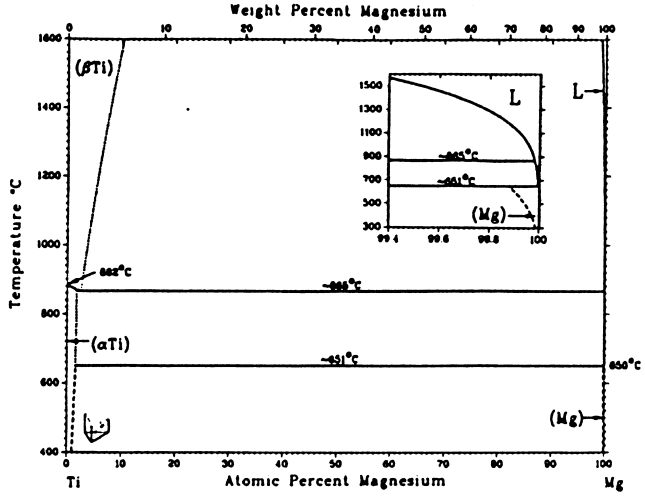

(c) Mg–Ti

Fig. 1. Phase diagrams for Mg–Ni, Ti–Ni and Mg–Ti systems.

it is considered that such a process can reduce substantially the production cost of nickel–metal-hydride (Ni–MH) batteries.

Mg_2Ni and TiNi are the intermetallic hydrogen-storage alloys that we wish to synthesize. Mg_2Ni is chosen because of its high hydrogen-storage capacity, but its degradation is very serious [6]. TiNi has good corrosion resistance, but suffers from an activation problem. Wakao et al. [7] reported that the TiNi electrode alloy has a discharge capacity of 270 mAh g^{-1}. Titanuim is selected because of its good corrosion-resistance. It has also has a high binding energy with Ni which similar to that of Mg with Ni. There is no binding between Mg and Ti. It is thought that a composite alloy of Mg_2Ni and TiNi may be produced easily by a mechanical alloying process without the formation of unnecessary phases. This possibility is supported by the phase diagrams for the Mg-Ni, Ti-Ni and Mg-Ti systems (see Fig. 1) [8].

In this paper, the mechanical alloying of elemental powders of Mg, Ni and Ti are studied to synthesize A_2B-type Mg_2Ni and AB-type TiNi composite alloys. A study is also made of the electrochemical properties of the new composite alloys in comparison with those of Mg_2Ni ball-milled under the same conditions.

2. Experimental

Mechanical alloying was carried out using a SPEX 8000-D ball miller. The starting materials for ball milling were elemental powders of Mg (99.8%), Ni (99.9%) and Ti (99.9%). These materials were placed in a hardened steel vial together with two steel balls of 12.70 mm diameter and four of 6.35 mm diameter. The ratio of the Mg, Ni, Ti elemental powders was 2:2:1 and is intended to yield a ratio of Mg_2Ni to TiNi of 1:1. The weight ratio of the ball to powder ratio was 10:1. Handling was done in an argon-filled glove-box to prevent oxidation of the powders.

The structures of the as-milled powders were characterized by X-ray diffraction (XRD) analysis (Rigaku D-Max3000) using Cu Kα (λ=1.5418 Å). Microstructural studies were performed by means of a scanning electron microscope (SEM) with an Energy-Dispersive X-ray Spectrometer (EDS).

The alloy powders were mixed with electrolytic Ni powder in a weight ratio of 1:2. They were then mechanically pressed into a pellet of 10 mm diameter on a nickel mesh under a pressure of 5 t cm^{-2} to produce the working electrodes. Electrochemical measurements were conducted in a half-cell which consisted of the composite metal hydride as a working electrode, a platinum counter electrode, and a Hg/HgO reference electrode in 6 M KOH and 1 M $LiOH{\cdot}H_2O$ electrolyte. Cycle tests were performed at 30°C using an automatic galvanostatic charge–discharge unit (Maccor series 4000) at a constant current density of 10, 30, 50 or 100 mA g^{-1}. The discharge cut-off potential was set at −0.60 V with respect to the reference electrode. The resting time between charge and discharge was 5 min.

3. Results and discussions

3.1. Analysis of structure evolution

X-ray diffraction patterns of ball-milled powders with milling times of 15, 20 and 25 h are shown in Fig. 2. It is seen that composite alloys with Mg_2Ni and TiNi phases are formed after 15 h of milling. At lower milling times, the Mg-Ti-Ni ternary system existed as an elemental state. The two phases are maintained with further milling up to 20 h. There is no change in the Mg_2Ni peaks, but the peak intensity of the TiNi phase increases. This result shows that the alloying process of the TiNi phase continues to 20 h. By contrast, Mg_2Ni has already reached a stable state after l5 h of milling. The reason why Mg_2Ni is formed earlier than TiNi is considered to be related to the diffusivity difference between Mg and Ti. The atomic radius of Mg and Ti is 1.72 and 2.0 Å, respectively. Generally, the lower the atomic radius of a element, the higher is the diffusivity. Therefore, the binding of Mg to Ni is faster than that to Ti is, and therefore, Mg_2Ni is formed at an earlier stage. After 25 h of ball-milling, peaks for $TiNi_3$, which does not have a hydrogen-absorption capability, are also observed. The enthalpy

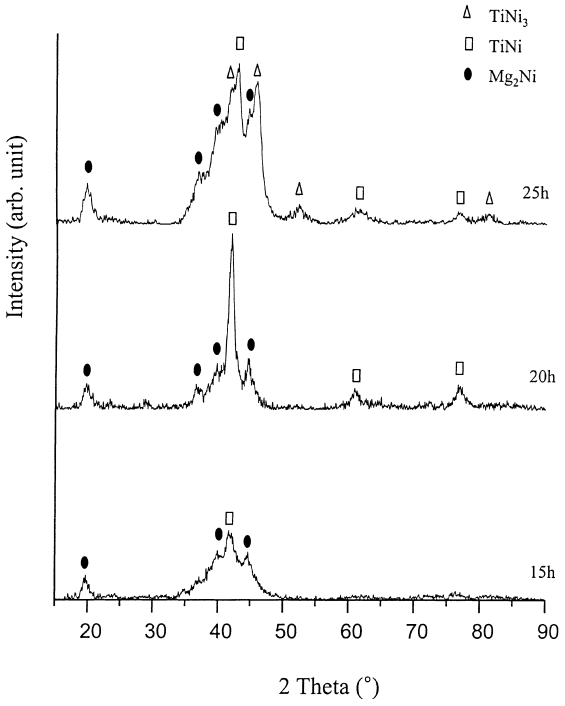

Fig. 2. XRD patterns of ball-milled powders prepared with different milling times.

of formation of TiNi and $TiNi_3$ is −67.781 and −138.909 kJ/mol, respectively, at 298.15 K. With more than 20 h of milling, the TiNi phase is transformed to $TiNi_3$ which is thermodynamically more stable than TiNi. More detailed studies of this phenomenon (phase transformation of Mg-Ni-Ti ternary system with ball-milling time) is in progress. Since $TiNi_3$ is not a hydrogen-storage phase, the hydrogen absorption capacity will be decreased with milling times >20 h. The optimal milling time to prepare the composite metal-hydride electrode alloy is, therefore, considered to be 20 h.

3.2. Microstructure of composite alloy

The morphology of composite alloy powders ball-milled for 20 h is shown in Fig. 3(a). The powders have composite phases: smaller particles with a size of about 5 μm are attached to the surface of larger particles with a size about 30 μm, although not uniformly. The large particles are TiNi and the smaller ones are Mg_2Ni, as shown by EDS qualitative analysis. From cross-sectional examination of the powders (Fig. 3(b)), it is seen that two phases, namely, Mg_2Ni and TiNi, co-exist in powders ball-milled for 20 h. Mg_2Ni particles have a rough surface while TiNi partiches have a smooth surface. The size (about 25 μm) of Mg_2Ni is smaller than that (above 30 μm) of TiNi. These results indicate that Mg_2Ni particles in ball-milled powders can be grouped into two types: one is an attached state (composite type) on TiNi particles, the other is an island state (mixture type). Mg_2Ni particles in the composite alloy have a smaller size than in the mixture type.

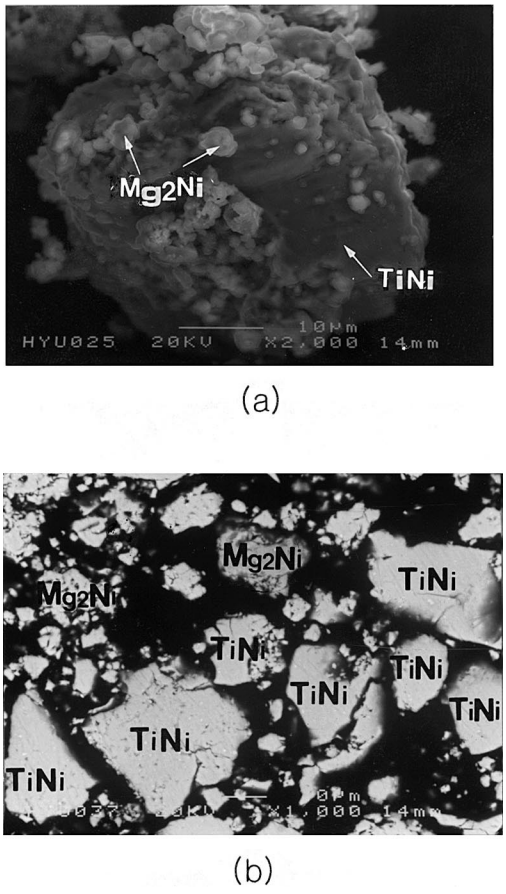

Fig. 3. Election micrographs of powders ball-milled for 20 h: (a) morphology (magnification 2000×); (b) cross-section (magnification 1000×).

In order to identify the distribution of Mg, Ni and Ti in Mg_2Ni and TiNi phase, EDS line-mapping was performed (in Fig. 4). The results show that little of the Ti is present as a solid-solution in the Mg_2Ni phase, while much of the Mg exists as such in the TiNi phase. Therefore, the distribution ratio of Mg_2Ni to TiNi phase is not 1:1 as intended, as is evident in Fig. 3(b).

Hellstern and Schultz [9] reported that only completely amorphous powders were obtained for the Ti–Ni system by mechanical alloying because of a large negative heat of mixing. In our work, however, a crystalline TiNi phase is formed by mechanical alloying. The discrepancy can be found in the tendency of Mg to dissolve in the TiNi phase. It is considered that a heat of mixing in Ti–Ni system is positively increased by addition of Mg in TiNi. Therefore, it is believed that this effect prevents amorphization of the TiNi system.

3.3. Electrochemical properties of composite alloy electrode

The discharge potential of the composite alloy electrode was compared with Mg_2Ni during the first cycle as shown in Fig. 5. The maximum discharge capacity of the electrode

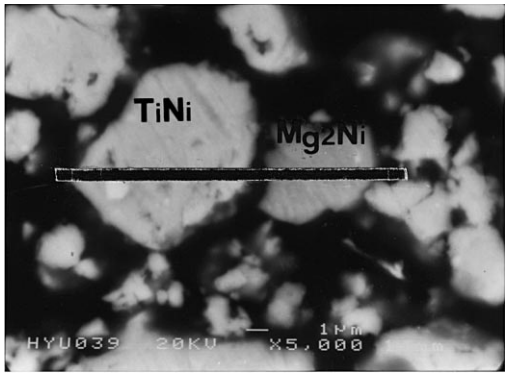

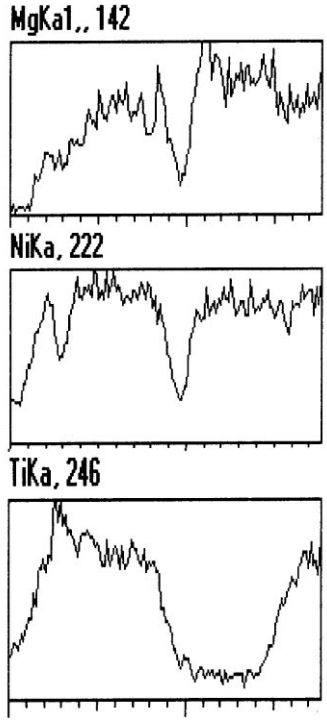

Fig. 4. EDS line-mapping for each element in TiNi and Mg_2Ni phases.

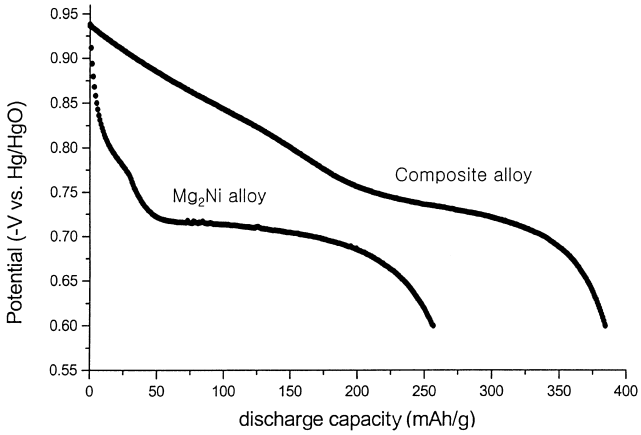

Fig. 5. Comparison of discharge potentials of composite alloy and Mg_2Ni at a current density of 10 mA g^{-1} during the first cycle.

and Mg_2Ni is about 380 and 255 mAh g^{-1}, respectively. There is a plateau region in both curves at almost the same voltage. The plateau are due to an electrochemical reaction of Mg_2Ni, i.e.

$$Mg_2NiH_x + xOH^- = Mg_2Ni + xH_2O + xe^- \quad \left(E_{plateau} = -0.72\,V \text{ versus } \frac{Hg}{HgO}\right) \quad (1)$$

It is also observed that the plateau region of Mg_2Ni with a single phase is wider than that of the composite alloy because the amount of Mg_2Ni is relatively larger in a single phase than in a composite alloy. Finally, the potential of the composite alloy electrode slowly decreases from −0.94 to −0.72 V. This is due to the existence of TiNi which, as in the case of Mg_2Ni, also contributes to the discharge capacity. Zuttel et al. [10] has reported that a discharge curve for two different phases should have two plateau. In our work, the plateau of Mg_2Ni in the composite electrode is slightly higher than −0.73 V, while the plateau of TiNi corresponding to a following electrochemical reaction

$$TiNiH_y + yOH^- = TiNi + yH_2O + ye^- \quad (2)$$

is not clearly observed. The slow slope of the discharge curve of the composite alloy electrode from −0.94 to −0.72 V suggests, however, that the narrow plateau of Eq. (2) might be in this region. The reason for a narrow plateau region with TiNi is that this alloy has a lower capacity compared with Mg_2Ni and requires several cycles to become activated. Geng et al. [11] have reported that Ti increases the anti-pulverization capability and leads to an increase in the cycling time required to activate the MH alloy electrode.

The discharge capacity of the 20 h ball-milled alloy electrode at different discharge current densities is shown in Fig. 6 as a function of cycle numbers. On the initial cycle, the discharge capacity of the composite alloy powder electrode at a discharge current density of 30, 50 and 100 mA g^{-1} is 213, 162 and 133 mAh g^{-1}, respectively. The decrease of discharge capacity with increasing current density after the first cycle is because the Mg_2Ni alloy does not have a high-rate capability. As the discharge capacity of TiNi is much lower than that of Mg_2Ni after the first cycle, as shown in Fig. 5, most of the discharge capacity in the composite alloy electrode is due to Mg_2Ni which does not need an activation process. As a result, an activation step is not observed in the composite alloy electrode. Rapid degradation of the composite alloy is also observed, as in the case of Mg_2Ni. This is because the corrosive Mg_2Ni surface is not fully covered with a TiNi phase. During electrochemical cycling, magnesium in the Mg_2Ni is easily oxidized in alkaline solution and a $Mg(OH)_2$ passive film is formed [6]. From these results, it can be concluded that the discharge process in the composite alloy electrode consists of two steps. Up to 40 cycles, most of the discharge capacity is due to Mg_2Ni while TiNi continues to be in an activation step. After 40 cycles, the TiNi phases, for which the activation has been completed, contribute to most of the discharge capacity because of the degradation of the Mg_2Ni phases. The discharge capacity of TiNi is higher after 40 cycles because of its activation characteristic. It is also shown that, regardless of discharge rate, the discharge capacity reaches a saturated value of about 100 mAh g^{-1} after 40 cycles.

At a discharge current density of l00 mA g^{-1}, the ratio of the discharge capacity to the maximum value in a composite alloy electrode was compared with that in single-phase Mg_2Ni electrode ball-milled for 20 h under the same conditions. The results are shown in Fig. 7. The cycle-life of the composite alloy electrode is better than that of Mg_2Ni. After 150 cycles, the ratio for the composite alloy electrode is about 55% while that for Mg_2Ni is below 10%. The greater cycle-life of the composite alloy electrode results from the activation process and the good corrosion resistance of TiNi.

A schematic diagram showing the role of the Mg_2Ni and TiNi alloy powders is presented in Fig. 8. Because Mg_2Ni particles are not completely covered with TiNi, a $Mg(OH)_2$ passive film is formed on the Mg_2Ni surface within several cycles. Therefore, hydrogen cannot diffuse towards the Mg_2Ni particles, only towards TiNi. Most of the composite

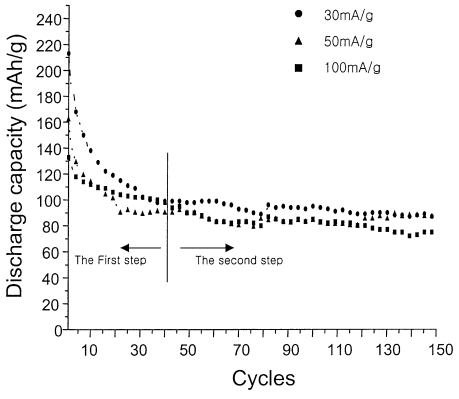

Fig. 6. Discharge capacity of 20 h ball-milled alloy electrode at different discharge currents as a function of cycle number.

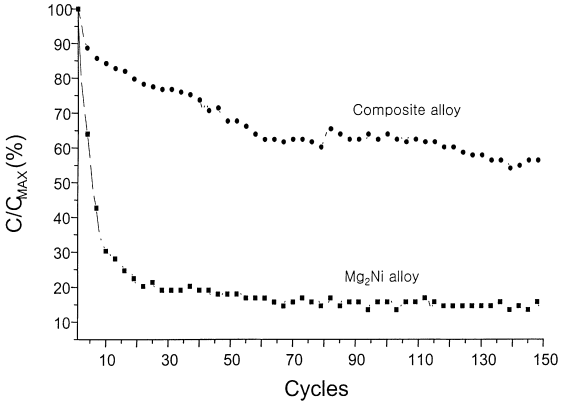

Fig. 7. Ratio of discharge capacity to maximum value between composite electrode and Mg_2Ni at a current density of 100 mA g^{-1}.

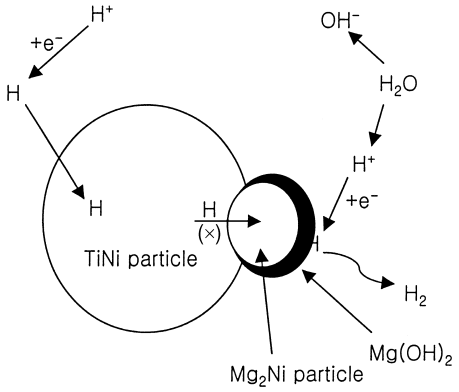

Fig. 8. Schematic diagram of role of Mg_2Ni and TiNi alloys powders in absorption of hydrogen.

electrode is not prepared by surface alloying, but by external pressure (cold-press). The interface between Mg_2Ni and TiNi in the composite electrode does not act as a diffusion layer. As a result, hydrogen which has diffused to the TiNi particles cannot move towards Mg_2Ni. The discharge capacity, therefore, is due only to the TiNi phase after 40 cycles. To improve the cycle-life, it is thought that Mg_2Ni should be fully surrounded by TiNi. To obtain this state, mechanical milling with variation of the ratio of Mg, Ni and Ti elemental powders and sintering of the cold-pressed pellet type electrode should be investigated.

4. Conclusions

A new composite metal hydride alloys which consist of Mg_2Ni and TiNi phases have been successfully synthesized by mechanical alloying of Mg, Ni and Ti elemental powders with a milling time of 20 h. EDS analyses reveal that little of the Ti is dissolved in the Mg_2Ni phase, while a large amount of Mg is dissolved in the TiNi phase. Thus, the amount of TiNi phase is more than that of Mg_2Ni. The discharge curve of the composite alloy electrode has two steps. On the first step, Mg_2Ni has a high discharge capacity, while TiNi is still in the activation process and makes little contribution. Thus, the discharge capacity of the composite alloy electrode is rapidly degraded within several cycles. On the second step, Mg_2Ni is degraded while the activation process of TiNi finishes and this phase contributes to the discharge capacity. Therefore, the cycle-life of the composite alloy electrode is longer than that of Mg_2Ni. After 150 cycles, the discharge capacity of the composite alloy electrode is 55% of the maximum value while that of Mg_2Ni is below 10%.

Acknowledgements

This work was supported by the Brain Korea 21 Project.

References

[1] N. Cui, B. Luan, H.J. Zhao, H.K. Liu, S.X. Dou, J. Alloys Comp. 240 (1996) 229–234.
[2] M. Terzieva, M. Khrussanova, P. Peshev, J. Alloys Comp. 267 (1998) 235–239.
[3] D. Cracco, A. Percheron-Guegan, J. Alloys Comp. 268 (1998) 248–255.
[4] D.J. Davidson, S.S. Sai Raman, O.N. Srivastava, J. Alloys Comp. 292 (1999) 194–201.
[5] S.M. Lee, H. Lee, J.S. Yu, G.A. Fateev, J.Y. Lee, J. Alloys Comp. 292 (1999) 258–265.
[6] N.H. Goo, J.H. Woo, K.S. Lee, J. Alloys Comp. 146 (3) (1999) 819–823.
[7] S. Wakao, Y. Younemura, H. Nakano, H. Shimada, J. Less-Common Met. 104 (1984) 365–373.
[8] T.B. Massalski, J.L. Murray, L.H. Bennett, H. Baker, L. Kacprzak, Binary Phase Diagrams, Vol.2, ASM.
[9] F. Hellstern, L. Schultz, Mater. Sci. Eng. 93 (1987) 213–216.
[10] A. Zuttel, F. Meli, D. Chartouni, L. Schlabach, F. Lichtenberg, B. Friedrich, J. Alloys Comp. 239 (1996) 175–182.
[11] M. Geng, J. Han, F. Feng, D.O. Northwood, J. Electrochem. Soc. 146 (1999) 3591–3595.